Changes in pattern formation and behavior in rotating Rayleigh-Bénard convection due to inhomogeneous thermal insulation

Janet Peifer

Onno Bokhove and Steve Tobias

University of Leeds

Department of Applied Mathematics & Leeds Institute for Fluid Dynamics

24 May, 2022

Overview

Introduction & Motivation

- Rayleigh-Bénard convection in molten planetary cores, affected by thermal conditions at the mantel (Mound & Davies, 2017)
- Explore the importance of thermal boundaries on fluid heat transport and temporal and spatial behaviour
- Can spatially inhomogeneous insulation cause time-independent behaviours and pin convection rolls in rapidly rotating system?

Figure: Image of the sun from National Geographic, a numerical simulation and a convection experiment at UCLA SpinLab.

Governing Equations

Boussinesq approximation applied to Navier Stokes equations:

$$\frac{D\boldsymbol{u}}{Dt} + 2\boldsymbol{\Omega} \times \boldsymbol{u} = -\frac{1}{\rho_0}\boldsymbol{\nabla} p + \alpha T \boldsymbol{g} + \nu \nabla^2 \boldsymbol{u}, \tag{1}$$

$$\boldsymbol{\nabla} \cdot \boldsymbol{u} = 0, \tag{2}$$

$$\frac{DT}{Dt} = \kappa \nabla^2 T. \tag{3}$$

Obtain non-dimensional equations by apply scalings such that,

$$t = \hat{t}\frac{d^2}{\kappa} \qquad \boldsymbol{x} = \hat{\boldsymbol{x}} d \qquad \boldsymbol{u} = \hat{\boldsymbol{u}}\frac{\kappa}{d} \qquad p = \hat{p}\frac{\kappa^2}{d^2} \qquad T = \hat{T}\Delta T, \tag{4}$$

where d is the height of the system.

Governing Equations

Eqs (1)-(3) now become non-dimensional:

$$\frac{D\boldsymbol{u}}{Dt} = -\nabla p + Pr\nabla^2\boldsymbol{u} - RaPrT\tilde{\boldsymbol{z}} - \frac{Pr}{Ek}\tilde{\boldsymbol{z}} \times \boldsymbol{u}, \tag{5}$$

$$\nabla \cdot \boldsymbol{u} = 0, \tag{6}$$

$$\frac{DT}{Dt} = \nabla^2 T. \tag{7}$$

With non-dimensional parameters Prandtl number, Rayleigh number, and Ekman number:

$$Pr = \frac{\nu}{\kappa} \qquad Ra = \frac{\alpha \Delta T d^3 g}{\nu\kappa} \qquad Ek = \frac{\nu}{2\Omega d^2} \tag{8}$$

Boundary Conditions

Top and Bottom ($z = z_1, z_0$):

- No-slip velocity: $\boldsymbol{u} = 0$
- Fixed temperature: $T(z_0, z_1) = 1, 0$

Sidewalls ($r = R$):

- No-slip velocity: $\boldsymbol{u} = 0$
- One of the following forms inhomogeneous heat flux:
  1. Positve/Negative:

$$\nabla T \cdot \boldsymbol{n} = \frac{\partial T}{\partial r} = \sum_{n=1}^{\infty} A_n \sin\left(f_n z\right) \sin\left(m_\theta \theta\right) \tag{9}$$

  2. Positive/Zero:

$$\frac{\partial T}{\partial r} = A_n \sin(\pi\left(z + 0.5\right))(1 + \sin(m_\theta \theta)) \tag{10}$$

A_n, f_n, and m_θ are constants

Numerical Simulations

- Nek5000: Spectral Element Method solver
- Cylindrical domain with aspect ratio $\Gamma = r/d = 0.7$
- Parameter range:
  $Pr = 0.7$
  $Ra \leq 10^8$
  $Ek \geq 10^{-5}$
- Initial condition: $\boldsymbol{u} = 0$ and $T = -z + 0.5$ with perturbation

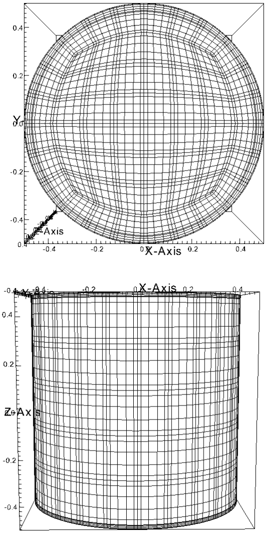

Positive/Negative BC on sidewall

$$\nabla T \cdot \boldsymbol{n} = \frac{\partial T}{\partial r} = \sum_{n=1}^{\infty} A_n \sin\left(f_n z\right) \sin\left(m_\theta \theta\right)$$

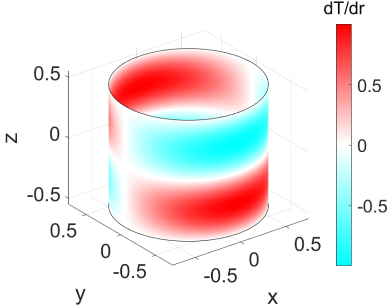

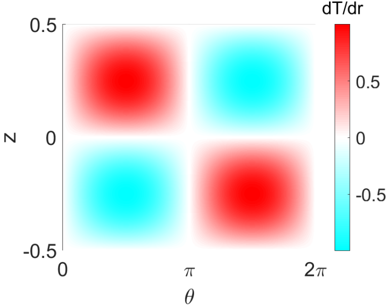

Heat flux at $r = R$ when $A_n = 1$, $f_n = 1$, and $m_\theta = 1$

$f_n = 1$ for all cases to simplify vertical deviation

Conducting Solution with P/N BC on sidewall

Solving Eqs (5-7) with Eq (9) for a state where $\boldsymbol{u} = 0$ and $dT/dt = 0$,

$$T(z, \theta, r) = \overline{T}(z) + T'(z, \theta, r)$$

$$\overline{T} = \frac{z}{z_0 - z_1} - \frac{z_1}{z_0 - z_1}, \qquad T' = \sum_{n=1}^{\infty} \frac{A_n}{\frac{\mathrm{d}I_m(Rf_n)}{\mathrm{d}r}} \sin(f_n z) \sin(m_\theta \theta) I_m(f_n r)$$

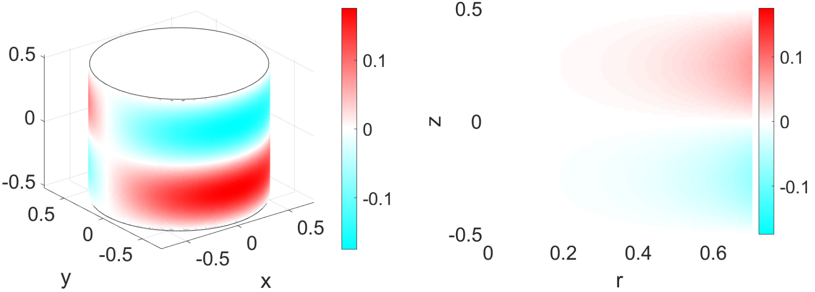

T' when $A_n = 1$, $f_n = 1$, and $m_\theta = 1$

Note I_m is a modified Bessel's function

Numerical Validation of P/N BC on sidewall

Use conducting solution (T_{cs}) and numerical simulation (T_{ns}) where $Ra < Ra_c$, so the system is conducting to validate numerical set up.
Quantified with $T^{\infty} = |max(T_{cs} - T_{ns})|$

Ek	Ra	m_θ	A_n	T^{∞}
∞	1	1	0.1	4×10^{-5}
			0.5	2×10^{-4}
		2	0.1	4×10^{-5}
10^{-3}	1	1	0.1	4×10^{-5}
10^{-4}	1	1	0.5	7×10^{-4}
			1	2×10^{-3}
		3	2	2×10^{-3}
10^{-5}	1	1	0.5	2×10^{-4}

T^{∞} increases as A_n increases due to the dI_m/dr term in the conducting solution, which is calculated numerically.
So as dr decreases, T^{∞} also decreases.
All results shown are calculated with $dr = 10^{-3}$.

Results of Positive/Negative BC on Sidewalls

$$\nabla T \cdot \boldsymbol{n} = \frac{\partial T}{\partial r} = \sum_{n=1}^{\infty} A_n \sin(f_n z) \sin(m_\theta \theta)$$

Azimuthal mode, m_θ is chosen in relation to the dominant mode, m_{UI} identified in the uniformly insulated (UI) system of the same Ek and Ra.
m_θ generally is either:

- $= 1$, to apply a larger wavelength at the sidewall than in the UI system, more similar to planetary cores (Mound & Davies, 2017) or
- $= m_{UI} > 1$, to investigate ability of lateral thermal boundary conditions to pin convection rolls (i.e.stop them from rotating about the domain)

Amplitude, A_n, is increased from 0.5 until effects are observed
Heat transport is measured by Nusselt number, $Nu = \frac{\Delta T}{(dT/dr)|_{z=z_1} d}$.

P/N BC on sidewall: Non-Rotating Example

$$Ek = \infty, \ Ra = 3 \times 10^5$$

UI system is chaotic with $m_{UI} = 1$. Apply $m_\theta = 1$ with $A_n = [0.5, 1, 2]$.

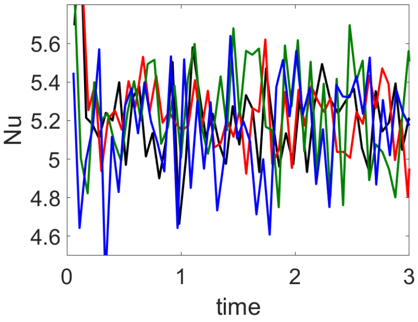

UI; $A_n = 0.5$; $A_n = 1$; $A_n = 2$

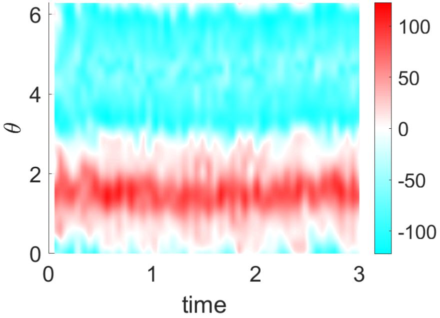

Hövmoller diagram of vertical velocity, w, for $A_n = 2$ taken at $z = 0.3$ and $r = 0.65$

Temporal behaviour is chaotic and dominant mode is $m = 1$ for all A_n

No significant change in behaviour due to heterogeneous sidewall insulation

P/N BC on sidewall: Weakly Rotating Example

$$Ek = 10^{-3},\ Ra = 4.8 \times 10^4$$

UI is time-independent with $m_{UI} = 3$. Apply $m_\theta = 1$ with $A_n = [0.5, 2, 3]$

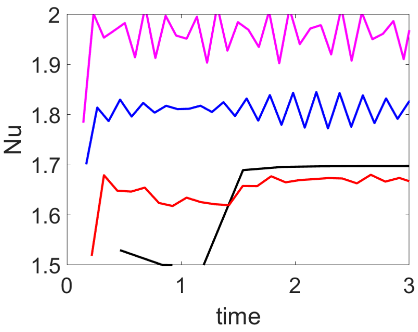

UI; $A_n = 0.5$; $A_n = 1$; $A_n = 3$

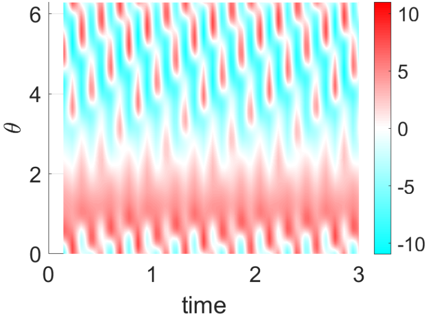

Hövmoller diagram of vertical velocity, w, for $A_n = 3$ taken at $z = 0.3$ and $r = 0.68$

$m_\theta = 1$ cause time-dependant behaviour and super-positions with $m_{UI} = 3$ mode, showing effects most strongly where applied $dT/dr > 0$.

P/N BC on sidewall: Weakly Rotating Example

$Ek = 10^{-3}$, $Ra = 4.8 \times 10^4$

UI is time-independent with $m_{UI} = 3$. Apply $m_\theta = 3$ with $A_n = [0.5, 2, 3]$

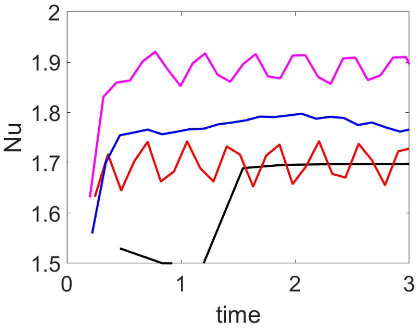

UI; $A_n = 0.5$; $A_n = 1$; $A_n = 3$

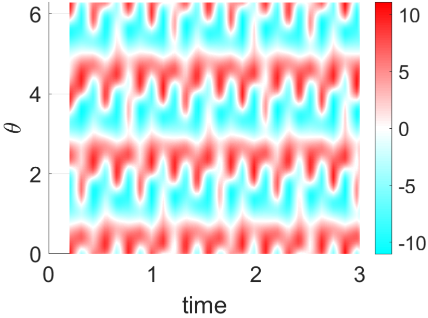

Hövmoller diagram of vertical velocity, w, for $A_n = 3$ taken at $z = 0.3$ and $r = 0.68$

$m_\theta = m_{UI} = 3$ causes oscillatory temporal behaviour. Convection rolls are pinned, but oscillate within range $\theta = 2\pi/m_\theta$.

P/N BC on sidewall: Rapidly Rotating Example

$$Ek = 10^{-5},\ Ra = 1.44 \times 10^{7}$$

UI is chaotic with small σ_{Nu} and $m_{UI} = 3$. Apply $m_\theta = 1$ & $A_n = [0.5, 1, 2]$

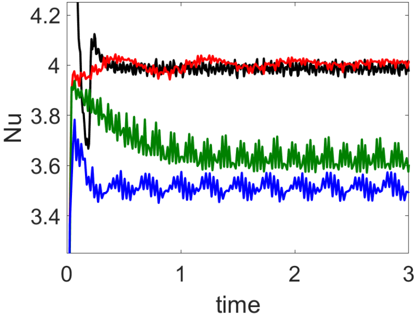

UI; $A_n = 0.5$; $A_n = 1$; $A_n = 2$

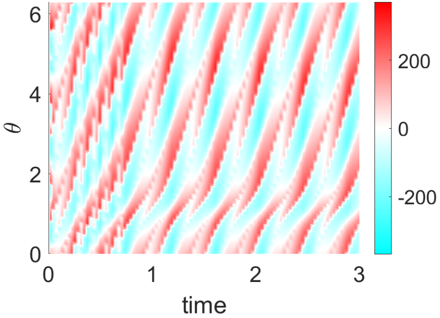

Hövmoller diagram of vertical velocity, w, for $A_n = 1$ taken at $z = 0.3$ and $r = 0.68$

As A_n increases, $\overline{Nu}$ decreases, and quasi-oscillatory temporal behaviour begins. Fluid rotates slower than UI, and slows further where $dT/dr > 0$

P/N BC on sidewall: Rapidly Rotating Example

$$Ek = 10^{-5},\ Ra = 1.44 \times 10^{7}$$

UI is chaotic with small σ_{Nu} and $m_{UI} = 3$. Apply $m_\theta = 3$ & $A_n = [0.5, 1, 2]$

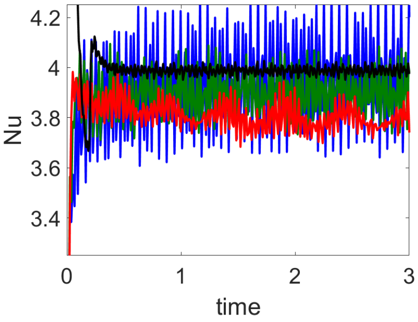

UI; $A_n = 0.5$; $A_n = 1$; $A_n = 2$

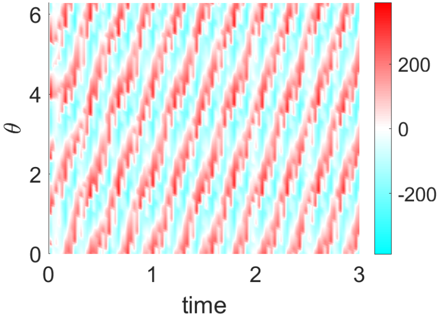

Hövmoller diagram of vertical velocity, w, for $A_n = 2$ taken at $z = 0.3$ and $r = 0.68$

As A_n increases, σ_{Nu} increases. For all A_n, fluid rotates slower than UI, upward and downward motion oscillate in strength 3 times in θ

P/N BC on sidewall: Discussion

- Vary heat flux in both z and θ to investigate planetary-core-like system:

$$\nabla T \cdot \boldsymbol{n} = \frac{\partial T}{\partial r} = \sum_{n=1}^{\infty} A_n \sin(f_n z) \sin(m_\theta \theta)$$

- Choose either $m_\theta = 1$, to approximate planetary cores
  - Fluid rotates slower where $dT/dr > 0$

  or $m_\theta = m_{UI}$, the dominant mode of the uniformly insulated case (UI) to pin convection rolls
  - pinned rolls within $\theta = 2\pi/m_\theta$ only when weakly rotating
- Generally, non-rotating systems are not affected by the inhomogeneous sidewall insulation.
- In rotating systems, the sidewall heat flux variation is observed to cause the system to become more time-dependant and make the fluid rotate about the domain, regardless of the temporal and spatial behaviour of the uniformly insulated system

2. Positive/Zero BC on sidewall

$$\frac{\partial T}{\partial r} = A_n \sin(\pi\,(z+0.5))(1+\sin(m_\theta \theta))$$

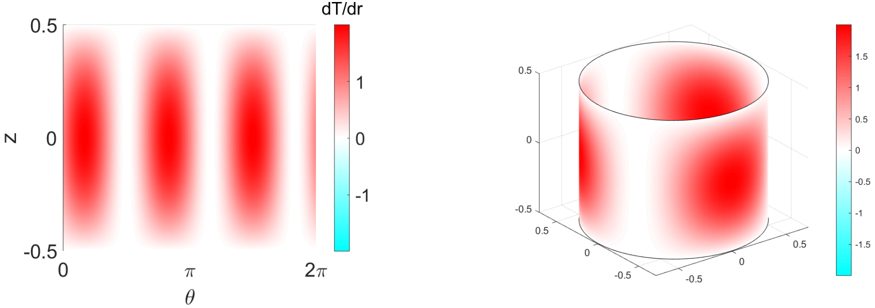

Heat flux at $r = R$ when $A_n = 1$,and $m_\theta = 3$

P/Z BC on sidewall: Heat Transport

Previous Nu definition not applicable. Redefine from Kunnen et al, 2008, $Nu = 1 + < wT >_V$, a volume average of the domain.

Following Hepworth, 2014, heat flux accounting is employed to validate numerical set-up. By integrating the heat equation, Eq(7), over the volume of the domain and applying the fixed temperature longitudinal and heterogeneous lateral (Eq (12)), we find that,

$$\int_0^R \int_0^{2\pi} \frac{\partial T}{\partial z} r \mathrm{d}\theta \mathrm{d}r|_{z=-Z} = \int_0^R \int_0^{2\pi} \frac{\partial T}{\partial z} r \mathrm{d}\theta \mathrm{d}r|_{z=Z} + 4RA_n \qquad (12)$$

Thus the difference in heat flux from the bottom to top of the system should be $4RA_n = 2.8A_n$.

P/Z BC on sidewall: Numerical Validation

We simulated a range of $Ek - Ra - m_\theta - A_n$ systems and measured the difference in heat flux between the top and bottom, $\Delta < \partial_z Tr >$, and divided by the A_n of each respective case.

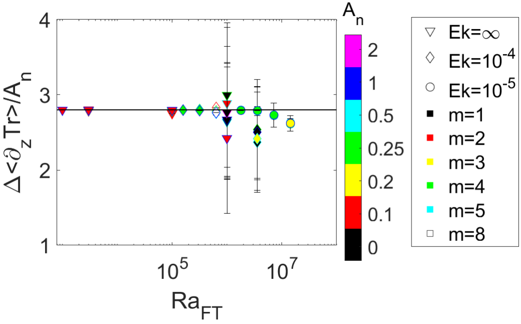

Ek, A_n, and *m* value are represented by the marker shape, edge colour, and fill colour, respectively. the solid line represents the expected value, 2.8. Error bars show the standard deviation.

Increase in *Ra* and decrease *Ek* case variation away from 2.8, likely due to increased time-dependence causing less certainty in heat flux measurements.

P/Z BC on sidewall: Non-rotating Example

$Ek = \infty$, $Ra = 3 \times 10^3$ UI is time-dependant with $m_{UI} = 1$. However, Positive/Negative BC results found no effect due to $m_\theta = m_{UI} = 1$. We apply $m_\theta = [2, 3]$ with $A_n = 1$.

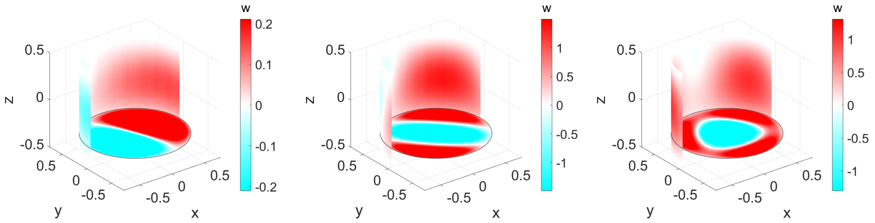

UI $\qquad m_\theta = 2 \qquad m_\theta = 3$

Vertical velocity, w, at $r = 0.69$, and $z = -0.3$

The dominant mode of the system becomes m_θ. The fluid motion in the bulk of the domain is affected, which was not observed in the P/N case.

P/Z BC on sidewall: Weakly Rotating Example

$Ek = 10^{-3}$, $Ra = 9.6 \times 10^4$

UI is time-independent with $m_{UI} = 2$. We apply $m_\theta = 1$ & $A_n = [0.5, 1, 2]$

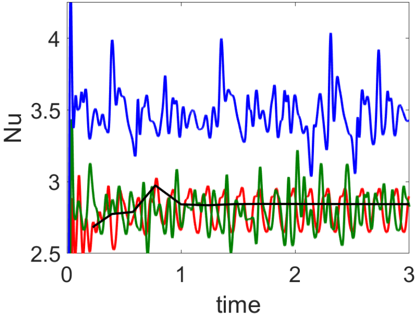

UI; $A_n = 0.5$; $A_n = 1$; $A_n = 2$

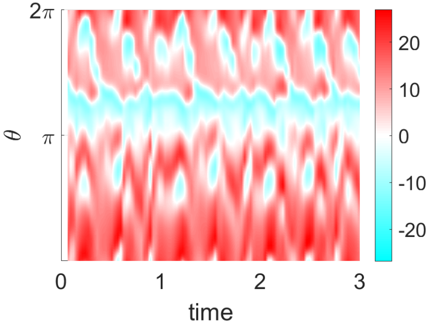

Hövmoller diagram of vertical velocity, w, for $A_n = 2$ taken at $z = 0.3$ and $r = 0.68$

All systems become chaotic, but $\overline{Nu}$ only increases when $A_n = 2$. One convection roll dominant, upward motion favoured where $dT/dr \neq 0$.

P/Z BC on sidewall: Weakly Rotating Example

$$Ek = 10^{-3},\ Ra = 9.6 \times 10^4$$

UI is time-independent with $m_{UI} = 2$. We apply $m_\theta = 2$ & $A_n = [1, 2]$

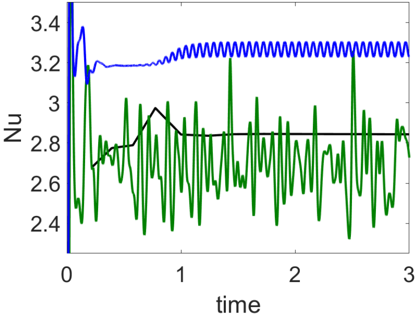

UI; $A_n = 1$; $A_n = 2$

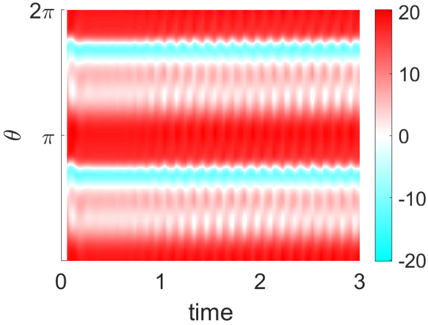

Hövmoller diagram of vertical velocity, w, for $A_n = 2$ taken at $z = 0.3$ and $r = 0.68$

Transition from chaos to oscillation as A_n increases, $\overline{Nu}$ also increases.
Upward motion strongly preferred where $dT/dr \neq 0$. Rolls pinned.

P/Z BC on sidewall: Rapidly Rotating Example

$Ek = 10^{-5}$, $Ra = 7.2 \times 10^6$

UI is oscillatory with $m_{UI} = 4$. We apply $m_\theta = 1$ & $A_n = [0.5, 1, 2]$.

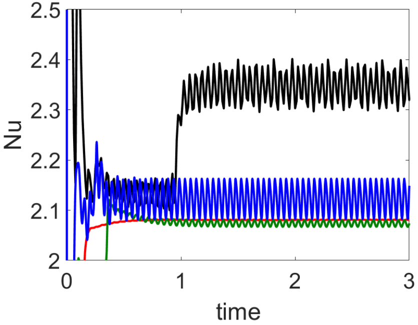

UI; $A_n = 0.5$; $A_n = 1$; $A_n = 2$

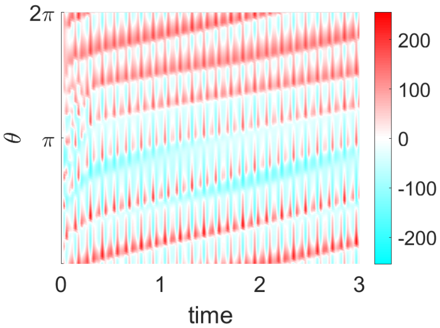

Hövmoller diagram of vertical velocity, w, for $A_n = 2$ taken at $z = 0.3$ and $r = 0.68$

$\overline{Nu}$ decreased with sidewall condition, amplitude of oscillation increases as A_n increases, strongest deformation of m_{UI} caused where $dT/dr \neq 0$

$$Ek = 10^{-5}, \; Ra = 7.2 \times 10^{6}$$

UI is oscillatory with $m_{UI} = 4$. We apply $m_\theta = 4$ & $A_n = [0.5, 1, 2]$.

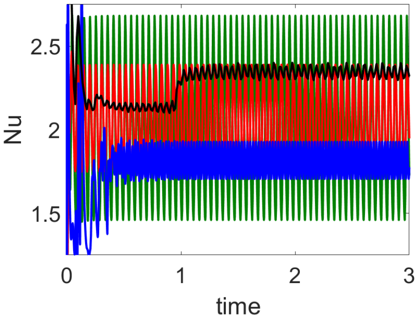

UI; $A_n = 0.5$; $A_n = 1$; $A_n = 2$

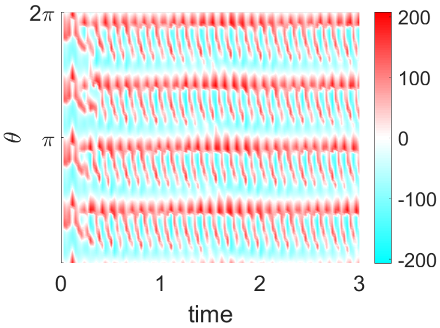

Hövmoller diagram of vertical velocity, w, for $A_n = 2$ taken at $z = 0.3$ and $r = 0.68$

$\overline{Nu}$ decreased as A_n increases. Convection rolls pinned where dT/dr strongest, with oscillations between $\theta = 2\pi/m_\theta$.

P/Z BC on sidewall: Discussion

- Define a thermal boundary condition which is $dT/dr > 0$ with a sinusoidal variation in z and θ:

$$\frac{\partial T}{\partial r} = A_n \sin(\pi (z + 0.5))(1 + \sin(m_\theta \theta))$$

- A Nu definition based on Kunnen, et al 2008 is defined
- Heat flux accounting following Hepworth, 2014 is followed to show that the difference in heat flux between the bottom and top of the system should be $2.8A_n$. Used to validate the numerical setup.
- Non-rotating: Convection rolls arrange into m_θ in the bulk of the fluid such that the centre of the system tends toward upward velocity
- Weakly rotating: $m_\theta = 1$ causes temporal chaos, $m\theta = m_{UI}$ the mode is pinned, for sufficient A_n.
- Rapidly rotating: $m_\theta = 1$ shows strongest deviation from m_{UI} where $\max(dT/dr) = 1$; $m_\theta = m_{UI}$ convection pinned where dT/dr is strongest with oscillation between; increasing A_n decreases $\overline{Nu}$.

Conclusions and Future Work

- Positive/Negative Thermal BC
  - Non-rotating systems not affected; Rotating systems become more time-dependant
  - $m_\theta = 1$ causes slow of fluid rotation where $dT/dr > 0$
  - $m_\theta = m_{UI}$ pins rolls but fluid oscillates within $\theta = 2\pi/m_\theta$
- Positive/Zero Thermal BC:
  - Non-rotating systems form m_θ number of rolls in the bulk
  - Rapidly rotating systems decrease in $\overline{Nu}$ as A_n increases
  - Rotating, for large A_n, pin rolls which oscillate between $\theta = 2\pi/m_\theta$
- Increasing the ratio between A_n and $\max(\boldsymbol{u})$ increases the effect on the system ($A_n \approx 2$ in Earth's core (Mound & Davies, 2017))
- Positive heat flux changes fluid behaviour more than negative heat flux variations - applicable to studies of planetary core dynamics, which have varying, positive, heat flux on boundaries
- In rotating systems, the application of $m_\theta = m_{UI}$ pins fluid everywhere- interesting potential experiment
- Future work: conduct experiments to verify results

References and Acknowledgements

1. NEK5000 Version 19.0. (2019). Argonne National Laboratory, Illinois.
2. Mound, J., and Davies, C. (2017). J. Fluid Mech.
3. Hepworth, B. (2014). PhD thesis. University of Leeds.

This work was undertaken on ARC3, part of the High Performance Computing facilities at the University of Leeds, UK.